NANO LETTERS

pubs.acs.org/NanoLett Letter

From Fano to Quasi-BIC Resonances in Individual Dielectric Nanoantennas

Elizaveta Melik-Gaykazyan,* Kirill Koshelev, Jae-Hyuck Choi, Sergey S. Kruk, Andrey Bogdanov, Hong-Gyu Park, and Yuri Kivshar*

Cite This: *Nano Lett.* 2021, 21, 1765−1771 Read Online

ACCESS | Metrics & More | Article Recommendations | Supporting Information

ABSTRACT: Sharp optical resonances in high-index dielectric nanostructures have recently attracted significant attention for their promising applications in nanophotonics. Fano resonances, as well as resonances associated with bound states in the continuum (BIC), have independently shown a great potential for applications in nanoscale lasers, sensors, and nonlinear optical devices. Here, we demonstrate experimentally a close connection between Fano and quasi-BIC resonances excited in individual dielectric nanoantennas. We analyze systematically the resonant response of AlGaAs nanoantennas pumped with a structured light in the near-infrared range. We trace a variation of the scattering spectrum that fully agrees with an analytical expression governed by a Fano parameter and observe directly a transition to a quasi-BIC resonance. Our results suggest a unified approach toward the analysis of sharp resonances in subwavelength nanostructures originating from strong coupling of optical modes that can provide high energy localization for enhanced light−matter interactions.

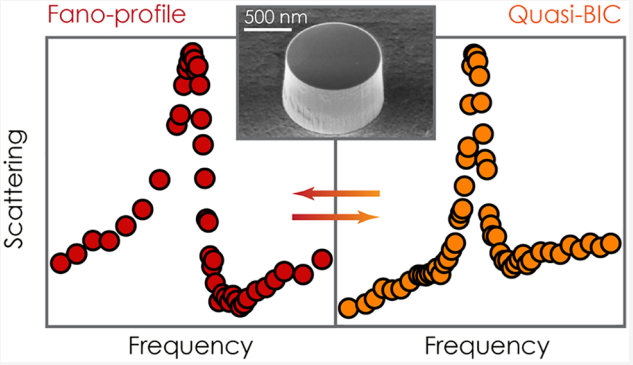

KEYWORDS: *Fano resonance, bound states in the continuum, vector beams, structured light, high-index dielectric nanoparticles, laser spectroscopy*

Dielectric structures hosting Mie resonances have recently become a vibrant research area, providing a versatile platform for engineering of electromagnetic properties at the nanoscale.[1,2] Compared to their plasmonic counterparts,[3] all-dielectric nanoparticles were shown to offer advanced functionalities[4,5] due to low absorption losses, the ability to support displacement currents in bulk, and simplicity of achieving artificial magnetic response.[6,7] Mie resonances in individual dielectric particles and their arrays have been widely explored for enhancing light−matter interactions at the subwavelength scale, including applications for optical harmonic generation,[8,9] quantum dot emission,[10] Raman scattering,[11] lasing,[12,13] colored images imprinting,[14] and enhancement of the near-field coupling effects.[15] Very recently, a prominent group of dielectric nanostructures that support the pronounced optical response associated with Fano resonances and the physics of bound states in the continuum (BICs) has drawn increased attention.[16] Considered as two unrelated resonant effects,[16] both Fano resonances and BICs were suggested as a vivid tool for a further increase in the efficiency of functional devices, especially for nonlinear and active applications.[17]

Fano resonances represent a universal wave interference phenomenon manifested as an asymmetric spectral feature with a specific line shape due to overlap of a narrow resonance with a "continuum" of modes, which in practice may be a much broader resonant mode. The famous Fano formula [see eq 1] describes the spectral response σ of the structure in dependence on the relative phase between the narrow and broad resonances, which is governed by Fano asymmetry parameter q:

$$\sigma(x) = \frac{(q + x)^2}{1 + x^2} \tag{1}$$

Here, $x = 2(\omega - \omega_0)/\gamma_0$ is the normalized frequency offset, ω_0 is the frequency of the narrow resonance, and γ_0 is its inverse lifetime. Originally predicted for autoionized states of electrons in the 1960s,[18] Fano resonances were later observed across many different branches of physics and attracted a lot of attention in optics as an efficient tool to engineer and control

Received: November 25, 2020
Revised: January 28, 2021
Published: February 4, 2021

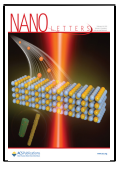

scattering of light in photonic devices.[19−21] The property of Fano resonances to provide a high field enhancement[19] in a narrow[22] spectral range allowed for the creation of Fano-resonant low-loss[23] and nonlinear metasurfaces,[24] enhanced third harmonic generation via magnetic Fano resonances[25] as well as detection of single protein monolayers with naked eye using plasmonic Fano resonances,[26] and other applications.

Very similar to Fano resonances, bound states in the continuum (BICs) were originally predicted for electrons in the beginning of the 20th century. They were proposed as peculiar electron states, which are localized despite the fact that their energies are larger than the zero energy of the potential.[27] Much later, BICs were rediscovered in photonics[28] and have attracted vivid interest for applications requiring high field enhancement. In practice, photonic BICs in large ensembles of particles manifest themselves as quasi-BICs—high-quality (high-Q) resonances weakly coupled to the radiative continuum due to interparticle destructive interference in the far-field. One of the prominent groups of quasi-BICs is accidental quasi-BICs, for which the coupling strength to the continuum can be controlled by tuning one of the structural parameters.[29] Very recently, accidental quasi-BICs were proposed and experimentally observed in optics and microwaves for individual subwavelength dielectric resonators of cylindrical shape.[30−33] In that case, sharp resonances were achieved by enabling destructive interference of several modes of the same symmetry in the far-field via a change of the resonator's aspect ratio. In a short time, the proposed high-Q nanocavities were shown to have a great potential for nonlinear nano-optics[32,34] and active nanophotonics.[35]

In this Letter, we experimentally uncover a fundamental link between the formation of quasi-BIC modes in individual dielectric nanoantennas and the peculiarities of the resonance asymmetry associated with the Fano line shape. A true BIC, being a theoretical construct characterized by an infinite Q factor, is associated with the collapse of a Fano resonance.[36,37] The connection between the appearance of quasi-BICs and unusual behavior of Fano resonances was noticed earlier[38,39] and discussed in several pioneering works for idealistic free-standing dielectric resonators.[30,31,33] However, transitions between two types of resonances have never been analyzed and observed in optics, where the presence of the substrate is inevitable.

In our study, we analyze the scattering spectra of a set of isolated AlGaAs nanodisks with variable diameters supporting a quasi-BIC, as schematically shown in Figure 1a−c. We consider excitation with a structured cylindrical beam in the near-infrared (near-IR) range. For the beam profile matching the quasi-BIC mode symmetry, we observe a clear transition of the line shape to a symmetric Lorentzian both in theory and experiment (see Figures 1d−f). We extract the Fano asymmetry parameter q from the simulated and measured spectra and observe that it diverges in the vicinity of the quasi-BIC regime (see Figure 1e), which gives a simple tool for its recognition by the naked eye as a completely symmetric resonant feature. For the symmetry-incompatible pump, we do not observe any spectral features, which confirms the importance of selective excitation for high-Q modes. We also study the dependence of the observed mode Q factor on the duration of the excitation pulse and reveal a characteristic dependence. Our results demonstrate that the mode interference mechanism in individual nanoantennas underpins the physics of Fano resonances as a phenomenon closely

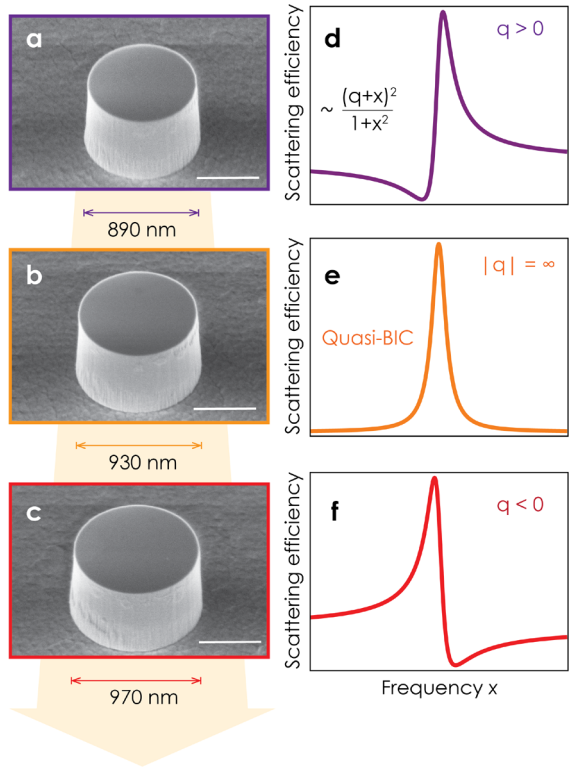

Figure 1. Schematic of the transition between Fano and quasi-BIC resonances in an individual dielectric nanoantenna. (a−c) Scanning electron microscope (SEM) images of individual AlGaAs nanoparticles with the height 635 nm and different diameters (a) 890, (b) 930, and (c) 970 nm, respectively. The nanodisks are trapezoidal in the vertical cross section, and the diameter is measured at the half-height. The scale bar is 500 nm. (d−f) Evolution of the spectral line shape [see eq 1] observed as a Fano resonance in the optical response of corresponding nanoparticles. x is the dimensionless frequency offset from a resonance. A change in the nanoparticle size leads to a (d) positive, (e) infinite, or (f) negative Fano parameter q.

associated with the strong mode coupling. Their interplay can be used for better energy localization in subwavelength optical structures and enhanced light−matter interaction.

The presence of a substrate introduces an additional channel of energy leakage, which leads to the decrease of local electromagnetic fields and the suppression of Q-factor values of optical modes supported by a nanoparticle. Therefore, we consider AlGaAs nanoparticles located on a multilayered substrate, as schematically shown in Figure 2a. We design the particles to support a high-Q mode with an azimuthally symmetric field profile associated with a quasi-BIC[32] with a Q factor of about 190 (see Supporting Information). The substrate consists of a 300 nm layer of ITO sandwiched between a 350 nm buffer layer of SiO_2 and a thick SiO_2 slab. The ITO layer is highly doped and is reflective at the pump frequency. Adjustment of the buffer layer thickness allows to compensate the parasitic diffraction to the substrate by additional interference of the quasi-BIC with its imaginary mirror image.[32,40−42] The nanoparticles are fabricated from an AlGaAs/AlInP/GaAs wafer using standard electron beam lithography with a sequential substrate transfer to the multilayered SiO_2/ITO/SiO_2 substrate (see Supporting Information). The scanning electron microscope (SEM) image of the fabricated structures is shown in Figure 2b. The nanoparticles are separated by 10 μm to prevent their coupling.

https://dx.doi.org/10.1021/acs.nanolett.0c04660
Nano Lett. 2021, 21, 1765−1771

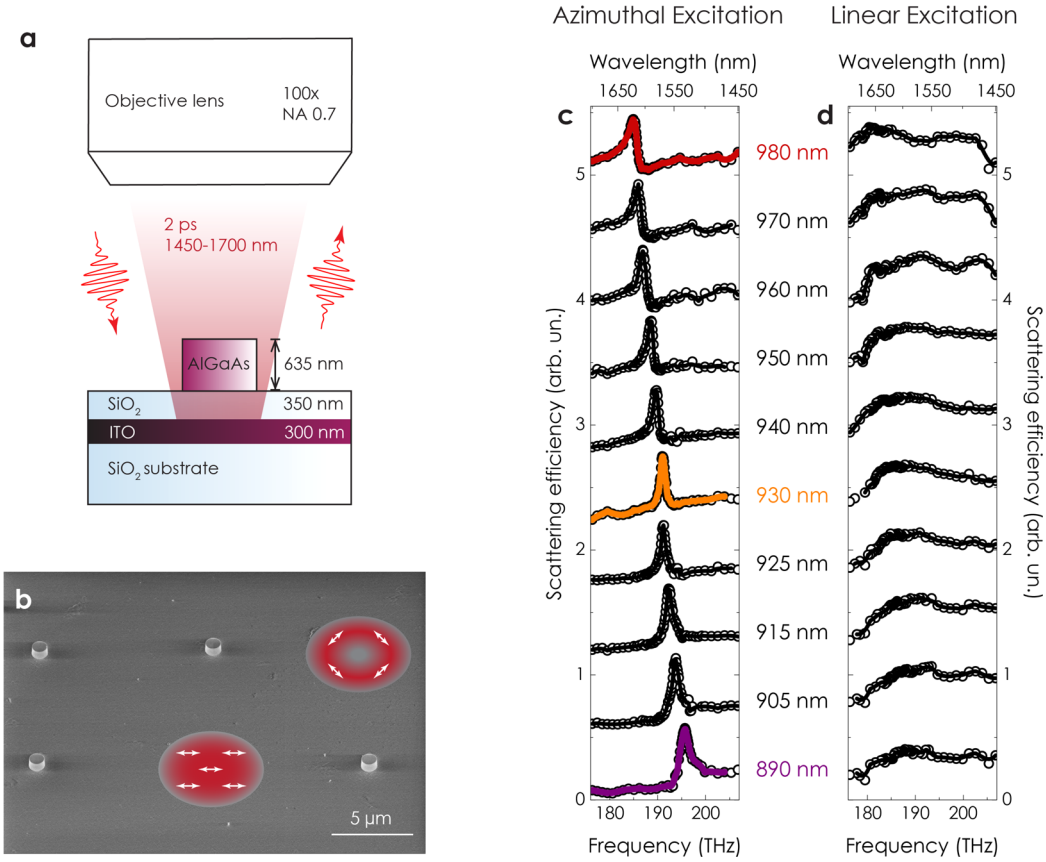

Figure 2. Measurements of resonant optical response of individual high-index nanoresonators. (a) Schematic of the structure and excitation setup, side view. (b) Scanning electron microscope image of several isolated nanoparticles. The red spots illustrate the in-plane field profiles of the linearly and azimuthally polarized pump beams with white arrows showing the polarization direction. (c, d) Measured reflectance spectra of nanoparticles in dependence on their diameter for (c) azimuthal and (d) linear excitation, respectively. Purple, orange, and red curves in panel c highlight three distinct types of peak asymmetry similar to Figure 1d–f.

They have the same height of 635 nm and varying diameters. The diameter of fabricated particles has a slight variation from the top to the bottom; thus, we consider the average diameter at the half-height, which spans across a 890–980 nm range.

We illuminate the fabricated nanoantennas with a focused pulsed laser beam (for details on the experimental setup, see Supporting Information). The schematic of the excitation setup is presented in Figure 2a. To pump the structures, we use the structured light in the form of a cylindrical vector beam[43] and consider two cases: azimuthal polarization[44] and linear polarization. Structured beams are widely used in nanoscale spectroscopy, and they can be implemented to inspect the nanostructure defects,[45,46] for selective excitation of nanoparticle multipoles,[47,48] or for spatial scanning of a nanoparticle structure to define the crystalline axes of its material.[49] The azimuthally polarized beams are shown to be the most efficient way to couple light to the quasi-BIC modes with an azimuthal field distribution inside a subwavelength resonator.[32,34,50]

We measure the reflected power from each particle in the spectral range of 1450–1700 nm and normalize it to the reflection from the substrate. We scan over multiple nanoantennas with different diameters and compare the variation of scattering spectra with the diameter change for azimuthal and for linear polarization of the incident laser beam. The experimentally measured spectra are shown in Figure 2c,d. For the azimuthal excitation (Figure 2c), we observe an isolated sharp resonant feature, which line shape is, in general, asymmetric and varies with the diameter of the nanoparticle. The peak asymmetry changes its sign from positive (purple, diameter 890 nm) to negative (red, diameter 980 nm); i.e., we vary the size of a nanoantenna within the range of 10%. The transition point, for which the peak becomes symmetric, is shown with an orange curve in Figure 2c. For the linear excitation, we do not observe any resonant features. The comparison of the scattering patterns for both azimuthal and linear excitation highlights the significance of a pump structuring to enable selective excitation of high-Q modes of nanoresonators.

To explain the experimental results, we perform full-wave simulations of the reflectance spectra. For numerical simulations, we use the finite-element-method solver in COMSOL Multiphysics in the frequency domain (for details on simulations, see Supporting Information). To compare the simulations with the measured spectra, we consider the experimental design as in Figure 2a, the azimuthally polarized pump, and the presence of the multilayered substrate. We calculate the reflected power coming through the 0.7 NA in the backward direction and normalize it on the reflectance from the substrate collected by the same aperture. The simulated reflection spectra for nanoparticles of different diameters are shown in Figure 3a. One can see that the peak shape evolves when the diameter changes from 890 to 980 nm.

To explain the change of peak shape, we derive the analytical solution for the scattering cross section of the nanoparticle. For

https://dx.doi.org/10.1021/acs.nanolett.0c04660
Nano Lett. 2021, 21, 1765–1771

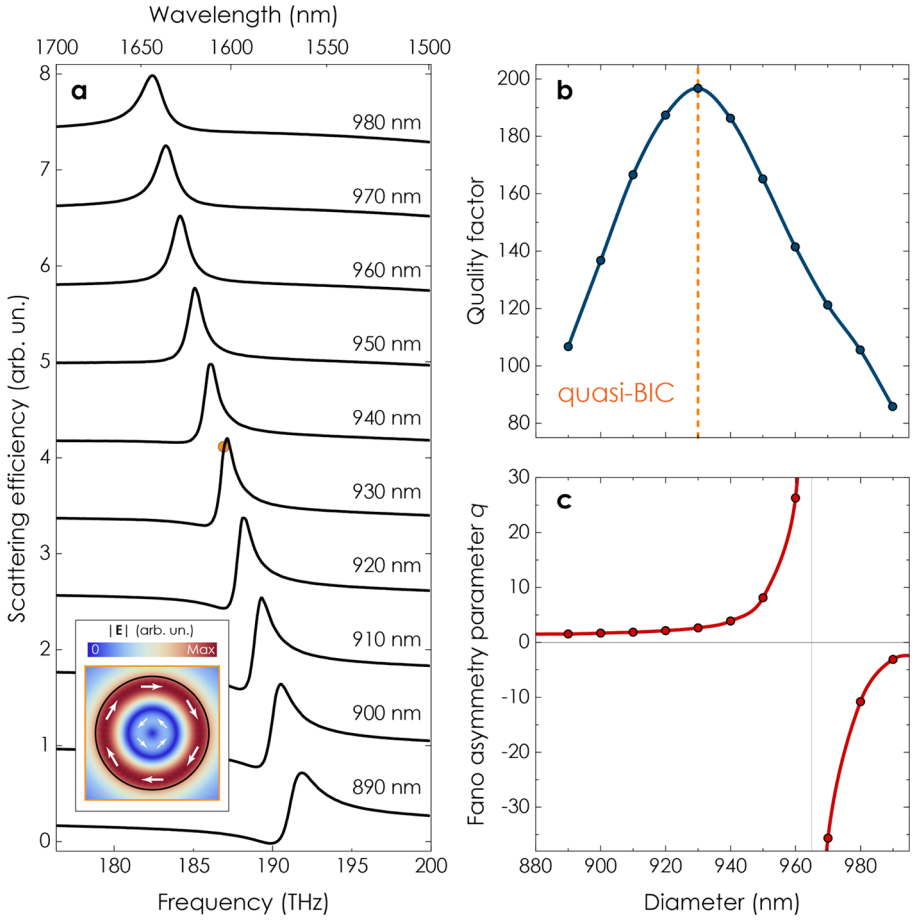

Figure 3. (a) Simulated backward reflectance spectra of a nanoantenna depending on the particle diameter. Inset shows a vector plot of the electric field at the half-height of the nanoparticle with a diameter of 930 nm at a resonant frequency of 186.9 THz. The black circle indicates a nanoparticle's edge; white arrows depict the polarization of the electric field inside the particle; the electric field contains an azimuthal component only. (b) Dependence of the Q factor extracted from the simulations on the disk diameter. The quasi-BIC is realized at a diameter of 930 nm. (c) Extracted values of the Fano asymmetry parameter q. Gray lines are a guide for the eyes. It can be seen that q diverges in the vicinity of the quasi-BIC.

analytical calculations, we assume the simplest case of a free-standing nanoparticle and linearly polarized excitation (for details, see Supporting Information). The analytical solution for the experimental design with a substrate and structured excitation can be derived in a similar manner. We expand the scattered field amplitude into the sum of independent terms, where each term corresponds to a resonant mode of the nanoantenna. The scattering cross section σ in the vicinity of resonance with frequency ω_0 and inverse lifetime γ_0 could be described (see Supporting Information) by the modified Fano formula:[31]

$$\sigma(x) = \frac{\sigma_0}{1+q^2}\frac{(q+x)^2}{1+x^2} + \sigma_{bg} \qquad (2)$$

Here, we use the same notations as for eq 1. The Fano asymmetry parameter can be expressed as $q = -\cot\Delta$, where Δ is the phase shift between the resonant mode and the background contribution coming from other modes and nonresonant scattering.[51] In sharp contrast to eq 1, the derived formula has additional terms, including the smooth peak envelope σ_0 and the background contribution σ_{bg}. Both σ_0 and σ_{bg} originate from the nonresonant contribution of other modes of the nanoparticle, which were not considered in eq 1. Also, in eq 2, the Fano asymmetry parameter appears explicitly in the denominator, which allows avoiding the divergence of σ for large q.

The analysis of eq 2 shows that the asymmetry parameter q strongly depends on the phase shift Δ: when Δ becomes zero, the asymmetry parameter diverges. Earlier analysis of free-standing high-index dielectric nanoparticles excited with a plane wave showed that, for the condition, $\Delta = 0$ can be fulfilled by tuning the resonance to the quasi-BIC regime.[31] To establish the relation between the peak asymmetry and the mode Q factor, we extract them from the simulated spectra as shown in Figure 3b,c (for details on the extraction procedure, see Supporting Information). The quasi-BIC with $Q = 185$ manifests itself for the nanoparticle with a diameter of 930 nm. As shown in Figure 3c, even for our complex structure with a structured excitation, the asymmetry parameter diverges in the vicinity of the quasi-BIC, which is in good agreement with earlier predictions;[30,31,33] any variation in the contribution from other eigenmodes of the fabricated nanoparticle and from a realistic multilayered substrate significantly affects the dependence of the asymmetry parameter q on the nanoparticle size.

Next, we analyze the relation between q and mode Q factor for the measured spectra using the same extraction procedure (see Supporting Information). Figure 4a shows that the peak

https://dx.doi.org/10.1021/acs.nanolett.0c04660
Nano Lett. 2021, 21, 1765−1771

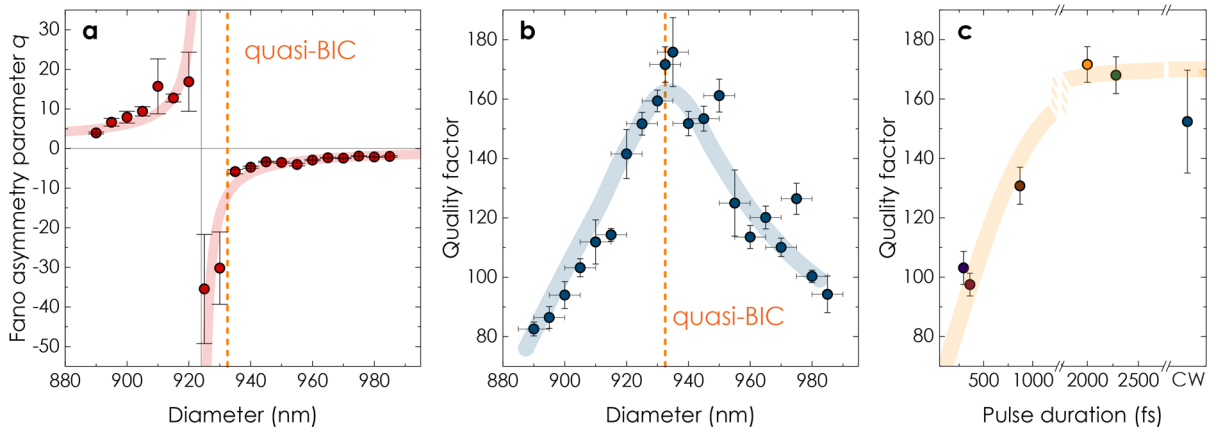

Figure 4. (a) The Fano parameter q and (b) observed Q factor extracted from the measured scattering spectra of individual AlGaAs nanoparticles excited by an azimuthally polarized vector beam. The measurements are conducted for the laser pulse duration of 2 ps. The orange vertical line depicts the location of the quasi-BIC mode. (c) Dependence of the observed quasi-BIC Q factor extracted from the measurements on the excitation pulse duration. The observed Q factors are measured for the excitation with the pulse duration of 295 fs (purple circle), 360 fs (wine), 870 fs (brown), 2.00 ps (orange), and 2.28 ps (green), respectively, and for a continuous-wave excitation regime (blue). Error bars determine the accuracy of a spectral line shape fitting procedure. The thick solid line is a guide for an eye, following the dependence in eq 3.

transforms to a symmetric Lorentzian for a diverging q for a diameter of about 925 nm, which is in the narrow vicinity of the quasi-BIC regime. As shown in Figure 4b, the experimentally measured dependence of the Q factor on the nanoantenna size demonstrates the maximal value of about 175 at a diameter of 930 nm, which in good agreement with the simulation results (see Figure 3b). The agreement between the condition of quasi-BIC formation and Fano parameter divergence in the experiment is even better than that in numerical simulations. This criterion of the transformation of an asymmetry parameter has also demonstrated numerically[52] and experimentally[53] for so-called superlattices supporting the optical modes associated with the physics of BIC.[28]

We further bring into consideration the importance of temporal coupling to high-Q nanoresonators. We pump the nanoparticle supporting the quasi-BIC and vary the duration of an optical pulse from a sub-ps to a continuous-wave regime, while tracing the variation of the scattering spectrum. For each measurement, we extract the observed mode Q factor, as shown in Figure 4c. One can see that the explicitly observed resonant line width of the quasi-BIC mode depends strongly on the pulse duration. Qualitatively, the measured spectral line width represents the sum of the mode line width and the pulse line width. In this approximation, the observed quality factor Q will depend on the pulse duration as

$$Q = \frac{Q_{CW}}{1 + \sqrt{2}/(\gamma_0 \tau)} \tag{3}$$

where $Q_{CW} \simeq 175$ is the intrinsic mode Q factor, which can be reached in the continuous-wave regime, γ_0 is the mode line width, and τ is the pulse full-width-at-half-maximum duration. Equation 3 and experimental measurements in Figure 4c demonstrate that, for shorter pulses, the measured Q factor is lower because their broad spectrum is inefficient for coupling to a narrow resonance. This effect of short pulse implementation has been observed experimentally in nonlinear up-conversion studies of Fano-resonant semiconductor metasurfaces.[24,54] The measured Q factors saturate toward the longer pulses.

In conclusion, our results illustrate experimentally, for the first time, the link between the physics of Fano resonances and quasi-BIC resonances excited in individual high-index dielectric nanoparticles in the near-infrared range. We have used selective excitation of the quasi-BIC mode with an azimuthally polarized pump matching the resonant mode profile and have shown the appearance of sharp resonant features in the simulated and measured reflectance spectra. We have extracted the values of mode Q factor and peak asymmetry from the simulated and measured data and have shown that the Fano asymmetry parameter diverges in close vicinity of the quasi-BIC regime. Finally, we have determined the relation between the measured line width of the quasi-BIC and the excitation pulse duration. Our findings prove a direct link between quasi-BIC states and Fano resonances as both phenomena are supported by similar physics. The established link paves the way toward a unified framework of sharp resonances in individual dielectric nanoresonators providing strong field enhancement for enhancing the light−matter interaction at the nanoscale.

■ ASSOCIATED CONTENT

Supporting Information

The Supporting Information is available free of charge at https://pubs.acs.org/doi/10.1021/acs.nanolett.0c04660.

Dielectric nanoantenna fabrication process; experimental setup for optical characterization; numerical simulations of scattering cross-sectional spectra; experimental data fitting procedure; mode analysis for an individual dielectric cylindrical nanoresonator; derivation of the modified Fano formula

(PDF)

■ AUTHOR INFORMATION

Corresponding Authors

Elizaveta Melik-Gaykazyan − *Nonlinear Physics Centre, Research School of Physics, Australian National University, Canberra 2601, Australia; Faculty of Physics, Lomonosov Moscow State University, Moscow 119991, Russia;* orcid.org/0000-0001-7633-2376; Email: elizaveta.melik-gaykazyan@anu.edu.au

https://dx.doi.org/10.1021/acs.nanolett.0c04660
Nano Lett. 2021, 21, 1765−1771

Yuri Kivshar − *Nonlinear Physics Centre, Research School of Physics, Australian National University, Canberra 2601, Australia;* orcid.org/0000-0002-3410-812X; Email: yuri.kivshar@anu.edu.au

Authors

Kirill Koshelev − *Nonlinear Physics Centre, Research School of Physics, Australian National University, Canberra 2601, Australia; Department of Physics and Engineering, ITMO University, St Petersburg 197101, Russia;* orcid.org/0000-0001-7475-1024

Jae-Hyuck Choi − *Department of Physics, Korea University, Seoul 02841, Republic of Korea*

Sergey S. Kruk − *Nonlinear Physics Centre, Research School of Physics, Australian National University, Canberra 2601, Australia;* orcid.org/0000-0003-0624-4033

Andrey Bogdanov − *Department of Physics and Engineering, ITMO University, St Petersburg 197101, Russia*

Hong-Gyu Park − *Department of Physics, Korea University, Seoul 02841, Republic of Korea; KU-KIST Graduate School of Converging Science and Technology, Korea University, Seoul 02841, Republic of Korea;* orcid.org/0000-0002-6375-0314

Complete contact information is available at: https://pubs.acs.org/10.1021/acs.nanolett.0c04660

Notes

The authors declare no competing financial interest.

■ ACKNOWLEDGMENTS

The authors thank Konstantin Ladutenko, Barry Luther-Davies, and Olivier Lee Cheong Lem for their technical assistance at various stages of the work development. This work was supported by the Australian Research Council, the Strategic Fund of the Australian National University, the National Research Foundation of Korea (NRF, grant no. 2020R1A4A2002828 funded by the Korean Government, MSIT), the Russian Ministry of Education and Science (14.W03.31.0008), and the Russian Foundation for Basic Research (19-02-00419 and 19-32-90106). E.M. acknowledges the support of the ACT Node of the Australian National Fabrication Facility in carrying out this research. K.K. and A.B. acknowledge support from the Foundation for the Advancement Theoretical Physics and Mathematics BASIS. H.-G.P. acknowledges support from the Samsung Research Funding & Incubation Center of Samsung Electronics (SRFC-MA2001-01).

■ REFERENCES

(1) Arbabi, A.; Horie, Y.; Bagheri, M.; Faraon, A. Dielectric metasurfaces for complete control of phase and polarization with subwavelength spatial resolution and high transmission. *Nat. Nanotechnol.* **2015**, *10*, 937−943.

(2) Kuznetsov, A. I.; Miroshnichenko, A. E.; Brongersma, M. L.; Kivshar, Y. S.; Luk'yanchuk, B. Optically resonant dielectric nanostructures. *Science* **2016**, *354*, aag2472.

(3) Schuller, J. A.; Barnard, E. S.; Cai, W.; Jun, Y. C.; White, J. S.; Brongersma, M. L. Plasmonics for extreme light concentration and manipulation. *Nat. Mater.* **2010**, *9*, 193−204.

(4) Staude, I.; Schilling, J. Metamaterial-inspired silicon nanophotonics. *Nat. Photonics* **2017**, *11*, 274−284.

(5) Kruk, S.; Kivshar, Y. Functional meta-optics and nanophotonics governed by Mie resonances. *ACS Photonics* **2017**, *4*, 2638−2649.

(6) Kuznetsov, A. I.; Miroshnichenko, A. E.; Fu, Y. H.; Zhang, J.; Luk'Yanchuk, B. Magnetic light. *Sci. Rep.* **2012**, *2*, 492.

(7) Evlyukhin, A. B.; Novikov, S. M.; Zywietz, U.; Eriksen, R. L.; Reinhardt, C.; Bozhevolnyi, S. I.; Chichkov, B. N. Demonstration of magnetic dipole resonances of dielectric nanospheres in the visible region. *Nano Lett.* **2012**, *12*, 3749−3755.

(8) Shcherbakov, M. R.; Neshev, D. N.; Hopkins, B.; Shorokhov, A. S.; Staude, I.; Melik-Gaykazyan, E. V.; Decker, M.; Ezhov, A. A.; Miroshnichenko, A. E.; Brener, I.; Fedyanin, A. A.; Kivshar, Y. S. Enhanced third-harmonic generation in silicon nanoparticles driven by magnetic response. *Nano Lett.* **2014**, *14*, 6488−6492.

(9) Liu, S.; Sinclair, M. B.; Saravi, S.; Keeler, G. A.; Yang, Y.; Reno, J.; Peake, G. M.; Setzpfandt, F.; Staude, I.; Pertsch, T.; Brener, I. Resonantly enhanced second-harmonic generation using III−V semiconductor all-dielectric metasurfaces. *Nano Lett.* **2016**, *16*, 5426−5432.

(10) Rutckaia, V.; Heyroth, F.; Novikov, A.; Shaleev, M.; Petrov, M.; Schilling, J. Quantum dot emission driven by Mie resonances in silicon nanostructures. *Nano Lett.* **2017**, *17*, 6886−6892.

(11) Zograf, G. P.; Ryabov, D.; Rutckaia, V.; Voroshilov, P.; Tonkaev, P.; Permyakov, D. V.; Kivshar, Y.; Makarov, S. V. Stimulated Raman scattering from Mie-resonant subwavelength nanoparticles. *Nano Lett.* **2020**, *20*, 5786−5791.

(12) Ha, S. T.; Fu, Y. H.; Emani, N. K.; Pan, Z.; Bakker, R. M.; Paniagua-Domínguez, R.; Kuznetsov, A. I. Directional lasing in resonant semiconductor nanoantenna arrays. *Nat. Nanotechnol.* **2018**, *13*, 1042−1047.

(13) Tiguntseva, E.; Koshelev, K.; Furasova, A.; Tonkaev, P.; Mikhailovskii, V.; Ushakova, E. V.; Baranov, D. G.; Shegai, T.; Zakhidov, A. A.; Kivshar, Y.; Makarov, S. V. Room-temperature lasing from Mie-resonant nonplasmonic nanoparticles. *ACS Nano* **2020**, *14*, 8149−8156.

(14) Proust, J.; Bedu, F.; Gallas, B.; Ozerov, I.; Bonod, N. All-dielectric colored metasurfaces with silicon Mie resonators. *ACS Nano* **2016**, *10*, 7761−7767.

(15) Lepeshov, S.; Kivshar, Y. Near-field coupling effects in Mie-resonant photonic structures and all-dielectric metasurfaces. *ACS Photonics* **2018**, *5*, 2888−2894.

(16) Staude, I.; Pertsch, T.; Kivshar, Y. S. All-dielectric resonant meta-optics lightens up. *ACS Photonics* **2019**, *6*, 802−814.

(17) Kivshar, Y. All-dielectric meta-optics and non-linear nanophotonics. *Nat. Sci. Rev.* **2018**, *5*, 144−158.

(18) Fano, U. Effects of configuration interaction on intensities and phase shifts. *Phys. Rev.* **1961**, *124*, 1866.

(19) Luk'yanchuk, B.; Zheludev, N. I.; Maier, S. A.; Halas, N. J.; Nordlander, P.; Giessen, H.; Chong, C. T. The Fano resonance in plasmonic nanostructures and metamaterials. *Nat. Mater.* **2010**, *9*, 707−715.

(20) Khanikaev, A. B.; Wu, C.; Shvets, G. Fano-resonant metamaterials and their applications. *Nanophotonics* **2013**, *2*, 247−264.

(21) Limonov, M. F.; Rybin, M. V.; Poddubny, A. N.; Kivshar, Y. S. Fano resonances in photonics. *Nat. Photonics* **2017**, *11*, 543−554.

(22) Yu, Y.; Xue, W.; Semenova, E.; Yvind, K.; Mork, J. Demonstration of a self-pulsing photonic crystal Fano laser. *Nat. Photonics* **2017**, *11*, 81−84.

(23) Yang, Y.; Kravchenko, I. I.; Briggs, D. P.; Valentine, J. All-dielectric metasurface analogue of electromagnetically induced transparency. *Nat. Commun.* **2014**, *5*, 5753.

(24) Yang, Y.; Wang, W.; Boulesbaa, A.; Kravchenko, I. I.; Briggs, D. P.; Puretzky, A.; Geohegan, D.; Valentine, J. Nonlinear Fano-resonant dielectric metasurfaces. *Nano Lett.* **2015**, *15*, 7388−7393.

(25) Shorokhov, A. S.; Melik-Gaykazyan, E. V.; Smirnova, D. A.; Hopkins, B.; Chong, K. E.; Choi, D.-Y.; Shcherbakov, M. R.; Miroshnichenko, A. E.; Neshev, D. N.; Fedyanin, A. A.; Kivshar, Y. S. Multifold enhancement of third-harmonic generation in dielectric nanoparticles driven by magnetic Fano resonances. *Nano Lett.* **2016**, *16*, 4857−4861.

(26) Yanik, A. A.; Cetin, A. E.; Huang, M.; Artar, A.; Mousavi, S. H.; Khanikaev, A.; Connor, J. H.; Shvets, G.; Altug, H. Seeing protein monolayers with naked eye through plasmonic Fano resonances. *Proc. Natl. Acad. Sci. U. S. A.* **2011**, *108*, 11784−11789.
(27) von Neumann, J.; Wigner, E. P. Über merkwürdige diskrete Eigenwerte. *Phys. Z.* **1929**, *30*, 465−467.
(28) Hsu, C. W.; Zhen, B.; Stone, A. D.; Joannopoulos, J. D.; Soljačić, M. Bound states in the continuum. *Nat. Rev. Mater.* **2016**, *1*, 1−13.
(29) Friedrich, H.; Wintgen, D. Interfering resonances and bound states in the continuum. *Phys. Rev. A: At., Mol., Opt. Phys.* **1985**, *32*, 3231.
(30) Rybin, M. V.; Koshelev, K. L.; Sadrieva, Z. F.; Samusev, K. B.; Bogdanov, A. A.; Limonov, M. F.; Kivshar, Y. S. High-Q supercavity modes in subwavelength dielectric resonators. *Phys. Rev. Lett.* **2017**, *119*, 243901.
(31) Bogdanov, A. A.; Koshelev, K. L.; Kapitanova, P. V.; Rybin, M. V.; Gladyshev, S. A.; Sadrieva, Z. F.; Samusev, K. B.; Kivshar, Y. S.; Limonov, M. F. Bound states in the continuum and Fano resonances in the strong mode coupling regime. *Adv. Photon.* **2019**, *1*, 016001.
(32) Koshelev, K.; Kruk, S.; Melik-Gaykazyan, E.; Choi, J.-H.; Bogdanov, A.; Park, H.-G.; Kivshar, Y. Subwavelength dielectric resonators for nonlinear nanophotonics. *Science* **2020**, *367*, 288−292.
(33) Odit, M.; Koshelev, K.; Gladyshev, S.; Ladutenko, K.; Kivshar, Y.; Bogdanov, A. Observation of supercavity modes in subwavelength dielectric resonators. *Adv. Mater.* **2021**, *33*, 2003804.
(34) Carletti, L.; Koshelev, K.; De Angelis, C.; Kivshar, Y. Giant nonlinear response at the nanoscale driven by bound states in the continuum. *Phys. Rev. Lett.* **2018**, *121*, 033903.
(35) Mylnikov, V.; Ha, S. T.; Pan, Z.; Valuckas, V.; Paniagua-Domínguez, R.; Demir, H. V.; Kuznetsov, A. I. Lasing action in single subwavelength particles supporting supercavity modes. *ACS Nano* **2020**, *14*, 7338−7346.
(36) Fonda, L. Bound states embedded in the continuum and the formal theory of scattering. *Ann. Phys.* **1963**, *22*, 123−132.
(37) Kim, C. S.; Satanin, A. M.; Joe, Y. S.; Cosby, R. M. Resonant tunneling in a quantum waveguide: Effect of a finite-size attractive impurity. *Phys. Rev. B: Condens. Matter Mater. Phys.* **1999**, *60*, 10962−10970.
(38) Kamenetskii, E.; Sadreev, A.; Miroshnichenko, A. *Fano Resonances in Optics and Microwaves*; Springer: Cham, 2018.
(39) Koshelev, K.; Lepeshov, S.; Liu, M.; Bogdanov, A.; Kivshar, Y. Asymmetric metasurfaces with high−Q resonances governed by bound states in the continuum. *Phys. Rev. Lett.* **2018**, *121*, 193903.
(40) Xu, L.; Rahmani, M.; Zangeneh Kamali, K.; Lamprianidis, A.; Ghirardini, L.; Sautter, J.; Camacho-Morales, R.; Chen, H.; Parry, M.; Staude, I.; Zhang, G.; Neshev, D.; Miroshnichenko, A. E. Boosting third-harmonic generation by a mirror-enhanced anapole resonator. *Light: Sci. Appl.* **2018**, *7*, 1−8.
(41) Sugimoto, H.; Fujii, M. Broadband dielectric−metal hybrid nanoantenna: Silicon nanoparticle on a mirror. *ACS Photonics* **2018**, *5*, 1986−1993.
(42) Pidgayko, D. A.; Sadrieva, Z. F.; Ladutenko, K. S.; Bogdanov, A. A. Polarization-controlled selective excitation of Mie resonances in a dielectric nanoparticle on a coated substrate. *Phys. Rev. B: Condens. Matter Mater. Phys.* **2020**, *102*, 245406.
(43) Litchinitser, N. M. Structured light meets structured matter. *Science* **2012**, *337*, 1054−1055.
(44) Zhan, Q. Cylindrical vector beams: from mathematical concepts to applications. *Adv. Opt. Photonics* **2009**, *1*, 1−57.
(45) Neugebauer, M.; Woźniak, P.; Bag, A.; Leuchs, G.; Banzer, P. Polarization-controlled directional scattering for nanoscopic position sensing. *Nat. Commun.* **2016**, *7*, 11286.
(46) Bautista, G.; Kauranen, M. Vector-field nonlinear microscopy of nanostructures. *ACS Photonics* **2016**, *3*, 1351−1370.
(47) Melik-Gaykazyan, E. V.; Kruk, S. S.; Camacho-Morales, R.; Xu, L.; Rahmani, M.; Zangeneh Kamali, K.; Lamprianidis, A.; Miroshnichenko, A. E.; Fedyanin, A. A.; Neshev, D. N.; Kivshar, Y. S. Selective third-harmonic generation by structured light in Mie-resonant nanoparticles. *ACS Photonics* **2018**, *5*, 728−733.
(48) Manna, U.; Sugimoto, H.; Eggena, D.; Coe, B.; Wang, R.; Biswas, M.; Fujii, M. Selective excitation and enhancement of multipolar resonances in dielectric nanospheres using cylindrical vector beams. *J. Appl. Phys.* **2020**, *127*, 033101.
(49) Camacho-Morales, R.; Bautista, G.; Zang, X.; Xu, L.; Turquet, L.; Miroshnichenko, A.; Tan, H. H.; Lamprianidis, A.; Rahmani, M.; Jagadish, C.; Neshev, D. N.; Kauranen, M. Resonant harmonic generation in AlGaAs nanoantennas probed by cylindrical vector beams. *Nanoscale* **2019**, *11*, 1745−1753.
(50) Volkovskaya, I.; Xu, L.; Huang, L.; Smirnov, A. I.; Miroshnichenko, A. E.; Smirnova, D. Multipolar second-harmonic generation from high-Q quasi-BIC states in subwavelength resonators. *Nanophotonics* **2020**, *9*, 3953−3963.
(51) Alpeggiani, F.; Parappurath, N.; Verhagen, E.; Kuipers, L. Quasinormal-mode expansion of the scattering matrix. *Phys. Rev. X* **2017**, *7*, 021035.
(52) Kim, S.; Kim, K.-H.; Cahoon, J. F. Optical bound states in the continuum with nanowire geometric superlattices. *Phys. Rev. Lett.* **2019**, *122*, 187402.
(53) Liu, Z.; Xu, Y.; Lin, Y.; Xiang, J.; Feng, T.; Cao, Q.; Li, J.; Lan, S.; Liu, J. High-Q quasibound states in the continuum for nonlinear metasurfaces. *Phys. Rev. Lett.* **2019**, *123*, 253901.
(54) Vabishchevich, P. P.; Liu, S.; Sinclair, M. B.; Keeler, G. A.; Peake, G. M.; Brener, I. Enhanced second-harmonic generation using broken symmetry III-V semiconductor Fano metasurfaces. *ACS Photonics* **2018**, *5*, 1685−1690.

https://dx.doi.org/10.1021/acs.nanolett.0c04660
Nano Lett. 2021, 21, 1765−1771